https://doi.org/10.1186/s43074-020-00022-w

PhotoniX

REVIEW Open Access

Vacuum-ultraviolet photodetectors

Lemin Jia, Wei Zheng* and Feng Huang

* Correspondence: zhengw37@mail.sysu.edu.cn
State Key Laboratory of Optoelectronic Materials and Technologies, School of Materials, Sun Yat-sen University, Guangzhou 510275, China

Abstract

High-performance vacuum-ultraviolet (VUV) photodetectors are of great significance to space science, radiation monitoring, electronic industry and basic science. Due to the absolute advantages in VUV selective response and radiation resistance, ultra-wide bandgap semiconductors such as diamond, BN and AlN attract wide interest from researchers, and thus the researches on VUV photodetectors based on these emerging semiconductor materials have made considerable progress in the past 20 years. This paper takes ultra-wide bandgap semiconductor filterless VUV photodetectors with different working mechanisms as the object and gives a systematic review in the aspects of figures of merit, performance evaluation methods and research progress. These miniaturized and easily-integrated photodetectors with low power consumption are expected to achieve efficient VUV dynamic imaging and single photon detection in the future.

Keywords: Vacuum-ultraviolet detection, Ultra-wide bandgap semiconductors, Selective response

Introduction

Vacuum-ultraviolet (VUV) spectrum is known to be in the wavelength range of 10–200 nm [1, 2], where the ultraviolet light is strongly absorbed by oxygen in the air and can only propagate in a vacuum, and that is the origin of its name. High-sensitivity detection of VUV light is of great significance to space science (space exploration, cosmic physics, etc.), radiation monitoring (synchrotron radiation, free electron laser, etc.), electronic industry (semiconductor lithography, surface technology, etc.) and basic science (analysis instrument, spectral physics, etc.) as shown in Fig. 1.

It is well-known that the sun tends to cause aurora, magnetic storms and ionospheric disturbance on the earth [3–7] in a period of intense activity, which will affect human life and even bring serious attacks on the earth. For example, in the famous Carrington Event in 1859, the solar storm destroyed the first primitive power system, leading to severe fire accident in a large number of telegraph systems and getting them burnt down [8]. In the maximum solar spectrum of 2003 (solar storms struck the earth and induced powerful magnetic storms) and the minimum solar spectrum of 2008 [9], a significant difference can be observed in the VUV region, which indicates that VUV light detection is probably the most effective way to monitor space weather and track star evolution [10].

© The Author(s). 2020 **Open Access** This article is licensed under a Creative Commons Attribution 4.0 International License, which permits use, sharing, adaptation, distribution and reproduction in any medium or format, as long as you give appropriate credit to the original author(s) and the source, provide a link to the Creative Commons licence, and indicate if changes were made. The images or other third party material in this article are included in the article's Creative Commons licence, unless indicated otherwise in a credit line to the material. If material is not included in the article's Creative Commons licence and your intended use is not permitted by statutory regulation or exceeds the permitted use, you will need to obtain permission directly from the copyright holder. To view a copy of this licence, visit http://creativecommons.org/licenses/by/4.0/.

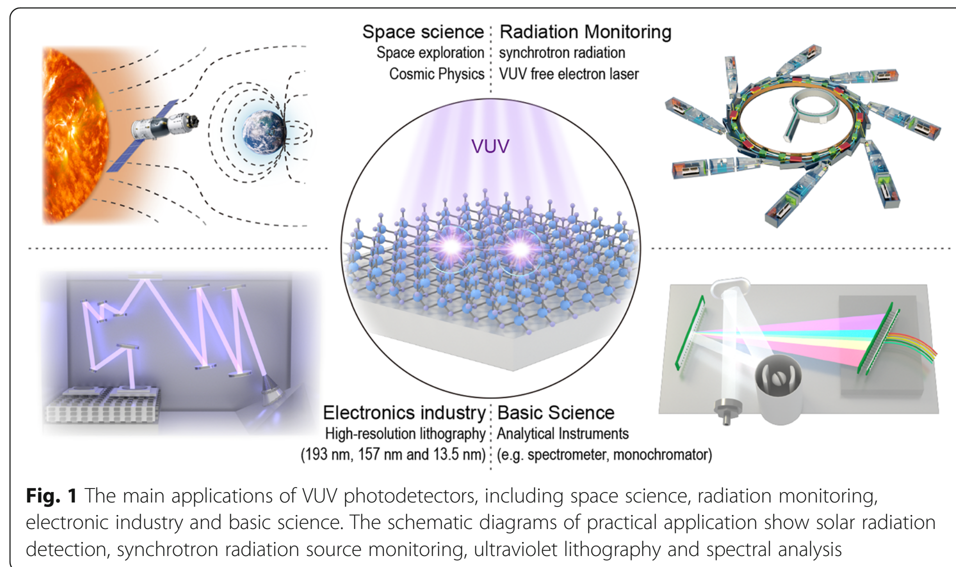

Fig. 1 The main applications of VUV photodetectors, including space science, radiation monitoring, electronic industry and basic science. The schematic diagrams of practical application show solar radiation detection, synchrotron radiation source monitoring, ultraviolet lithography and spectral analysis

As the most direct tool for studying the interaction between light and atoms, molecules and condensed matter, VUV light is involved in many fields of basic science such as spectroscopy and photochemistry, which has become an important driving force for the development of various VUV photodetectors. More importantly, high-performance VUV photodetectors are essential to high-resolution semiconductor lithography [11] (such as 193 nm and 157 nm excimer lithography, 13.5 nm extreme ultraviolet (EUV) lithography), synchrotron and free-electron lasers (FEL) beam monitors [12].

Due to the limitation of atmosphere and the lack of related technologies, it's difficult to carry out the researches on VUV photodetectors. At the end of the twentieth century, some solar-terrestrial physicists and cosmologists tried to load a combined system of Rowland chromatograph and microchannel plate [13, 14] on satellites for real-time solar VUV detection. However, these conventional detection systems require a driving voltage of several thousand volts, which imposes excessive burden of power supply on the operation of satellites. In the past 20 years, due to the advantages of miniaturization and ease of integration [15], VUV detectors based on the emerging ultra-wide bandgap (UWB) semiconductors have attracted researchers' attention. A typical case is in 2009 when an ultraviolet diamond detector was applied to space for the first time and the vacuum ultraviolet solar radiometer Large Yield Radiometer (LYRA) was released on the European Space Agency's PROBA2 [9, 16]. This on-board test first demonstrated the application potential of UWB semiconductor-based VUV photodetectors in solar physics research. Encouragingly, in the summer of 2018, NASA launched the first solar probe to complete the significant mission of exploring the mysteries of the sun at a distance of 7 million kilometers from its surface. A year later, the first research results of the Parker Solar Probe on the corona and solar wind were announced [17–20]. There is no doubt that the UWB semiconductor VUV detector definitely plays an indispensable role in this difficult task.

Photodetectors in the VUV region generally have to operate in a clean and ultra-high vacuum environment, and cannot interact or degrade in the presence of radiation. In

addition, low level of background noise is needed to help detect relatively weak signals. Silicon photodiodes originally designed for the visible spectrum range can be used in the VUV region [21–23], but the significant disadvantage lies in the inherent wide-band response from X-ray to near-infrared and radiation degradation. The direct method to fabricate highly-selective VUV detectors with high radiation hardness is to use UWB semiconductors [24]. Compared with the silicon-based detectors with relatively mature production technologies, UWB semiconductor-based detectors are still at a stage of rapid development, and significant improvements in terms of quantum efficiency, responsivity, response time, spectral response, and detection are required. Nevertheless, their absolute advantages in terms of VUV selective response and tolerance to harsh environments still attract a lot of interest from researchers [15, 25]. Their efforts like designing different device structures and studying different types or sizes of photosensitive materials to improve light absorption efficiency, carrier transmission efficiency and device lifetime have brought considerable development to UWB semiconductor-based VUV photodetectors and to the emergence of new VUV detection technologies.

In this review, we roughly divide UWB semiconductor detectors into three categories: photoconductive, photovoltaic, and avalanche based on the dominant working mechanism of devices in specific researches. Although the structure of the prepared device is clear, its actual working mechanism is often too complicated to be judged if without the help of experimental results. In a review published before, various VUV detection technologies such as photomultiplier tubes, scintillator detectors, Si-based photodetectors and gaseous detectors have been introduced [26]. This review will focus on the ultra-wide bandgap semiconductor-based filterless VUV photodetectors, especially the figures of merit under different working mechanisms, performance evaluation methods and research progress.

Quantifying the performance of VUV photodetectors

Basic indicators

The major physical mechanism of semiconductor photodetectors is photon absorption which changes the electrical properties of electronic systems. The performance of a photodetector depends on the optical absorption process, carrier transport and its interaction with the circuit system. The main performance indicators include quantum efficiency, responsivity, spectral response, response time, noise equivalent power and detectivity. But for VUV radiation, the radiation resistance of photodetectors, that is, the degree of decline in the above performance indicators after a certain amount of radiation, is also a figure of merit worthy of consideration and attention.

The internal quantum efficiency of photodetectors is defined as the number of carriers generated with per photon absorbed. In order to measure the number of carriers produced by each electron-hole pair, there is another widely-used concept called “photoconductive gain”, which depends on the carrier lifetime and the ratio of carrier transit time between the two electrodes. Generally, without considering the recombination loss, the internal quantum efficiency is equal to 1, but this value may be greater for photodetectors with internal gain mechanism. In practice, incomplete absorption will cause the number of photons absorbed by the detector to be less than that of

incident photons, and the external quantum efficiency (EQE) is thus defined as the ratio of the number of generated carriers to that of incident photons.

Responsivity is another important parameter to describe the photoelectric conversion efficiency of photodetectors, which is defined as the ratio of the output signal of photodetectors to the unit incident light power. According to the difference of various output signals, responsivity can be divided into the current one and voltage one. Most photodetectors are selectively responsive to spectra, which is called spectral response, namely a property that the responsivity varies with the wavelength of incident light. For a filterless VUV photodetector, the responsivity in the VUV region should be much greater than the long-wave region (or no response in the long-wave region).

In many fields of application, the response speed of photodetectors should be faster enough to meet the working requirements when compared with the data rate of digital transmission. Thus, response time is another important parameter of photodetectors. The response time of photoconductive detectors is determined by the carrier lifetime which is related to the characteristics of semiconductors. When the illumination stops, the carrier concentration will decay with time in a certain rule.

Noise equivalent power is an important parameter to describe the detection capability of photodetectors. Its value is equal to the incident light power when the output voltage of photodetectors is exactly equal to the output noise voltage. When the photodetector operates in a condition that the background flux is smaller than the light (signal) flux, its ultimate performance will be determined by the signal fluctuation limit. Detectivity is defined as the reciprocal of noise equivalent power, which reflects the detection capability of detectors more intuitively. Since detectivity is proportional to the square root of illuminated area of the detector and the square root of amplifier bandwidth, the concept of normalized detectivity is introduced to eliminate this effect. The larger the normalized detectivity is, the stronger the detector's ability to detect weak light will be.

Expression for photoresponsivity

For both photoconductive and photovoltaic detectors, photoresponsivity is the primary core evaluation indicator among all the parameters. In fact, this key parameter can be strictly described by mathematical formula if.with an ideal model.

For photoconductive detectors, the photoresponsivity depends on: 1) the intrinsic properties of photosensitive materials, such as carrier collection efficiency μτ (τ is the carrier lifetime, μ is the carrier mobility); 2) device structure, such as the spacing between positive and negative electrodes. Photoconductive gain (G) can be used as a bridge to deduce the specific expression. The current responsivity R_λ can be defined as $R_\lambda = I_{ph}/P_{in}$ (I_{ph} is the photocurrent, P_{in} is the input optical power), which can be specifically expressed by the following formula [27].

$$R_\lambda = \frac{\mu\tau V\eta e\lambda}{L^2 hc} = EQE\frac{e\lambda}{hc}$$

In this formula, η stands for quantum efficiency ($\eta = \eta_{abs}\eta_{trans}$, η_{abs}: light absorption efficiency; η_{trans}: charge transmission efficiency), V the driving voltage imposed on carriers, L the electrode spacing, e the electron charge, λ the wavelength and hc/λ the energy per photon. Therefore, the EQE of photoconductive devices can be described as EQE $=\eta$ G.

Absorption coefficient, carrier transfer and collection efficiency are three indicators positively correlated with photoresponsivity, which are mainly determined by photosensitive materials. Therefore, semiconductor materials with excellent photoelectric properties are the primary choice in the design of high-responsivity photodetectors. Furthermore, in the design of device structure, vertical structure has more advantages than the horizontal one in reducing the spacing between positive and negative electrodes.

As for photovoltaic detectors, the photoresponsivity can also be described by $R_\lambda = I_{ph}/P_{in}$. Generally speaking, the gain of photovoltaic detectors is 1, that is to say, the number of photo-generated electron-hole pairs equals to that of carriers contributing to the current. Therefore, the expression of photoresponsivity for photovoltaic detectors is $R_\lambda = \eta e\lambda/hc$, in which the EQE of photovoltaic devices is expressed as EQE $=\eta$. The analysis of the working mechanism of photovoltaic detectors mainly focuses on the carrier drift and diffusion processes. In theory, it can be deduced from simplified ideal models, such as Poisson equation and continuity equation; but in practice, the mechanism of devices tends to be much more complex because of the existence of defects in semiconductors and dislocations at heterojunctions. Therefore, in addition to the optimized design of device structure, the growth of high-quality semiconductor materials is also a decisive factor that influences the performance of photovoltaic detectors.

Balance between photoresponsivity and response time

For photoconductive detectors, external bias voltage is required for the device to work. In theory, there is no upper limit for R as well as for the corresponding external quantum efficiency. The photoresponsivity of the device is positively correlated with the response time: $R_\lambda \propto f(t)$, $R_\lambda = I_0 + I_s/P_{in}$, where I_0 refers to transient photocurrent and I_s is persistent photocurrent [28]. The longer the lifetime of trap state is, the larger the I_s and R_λ of the device will be, but at the same time, the recovery time of the device from on to off will also be longer [29].

In general, when photoconductive detectors absorb photons and generate electron-hole pairs, the majority of carriers (electrons) will have higher mobility with a shorter transit time than carrier lifetime; while the minority of carriers (holes) move slowly with a longer transit time than carrier lifetime. In this case, the electrons are quickly swept out of the detector, and the holes inside are redundant, and the other electrode needs to provide electrons to maintain electrical neutrality. Through such behavior, electrons can go back and forth for multiple times during the carrier lifetime, and the photodetector can thus obtain a larger gain, which is commonly understood as persistent photoconductivity. The longer the recombination life of the carriers is, the greater the responsivity of the photodetector will be. However, this mechanism will inevitably lead to an increase in switching response time, as shown in Fig. 2a, b.

Therefore, in practical application, it is necessary to make a trade-off between the two key indicators of responsivity and response time. The carrier lifetime is not only related to the properties of semiconductors, but also to the lifetime of trap states. For high-quality semiconductors with smooth surface and low defect density, when the illumination is stopped, carriers can recombine more rapidly, thus inhibiting the

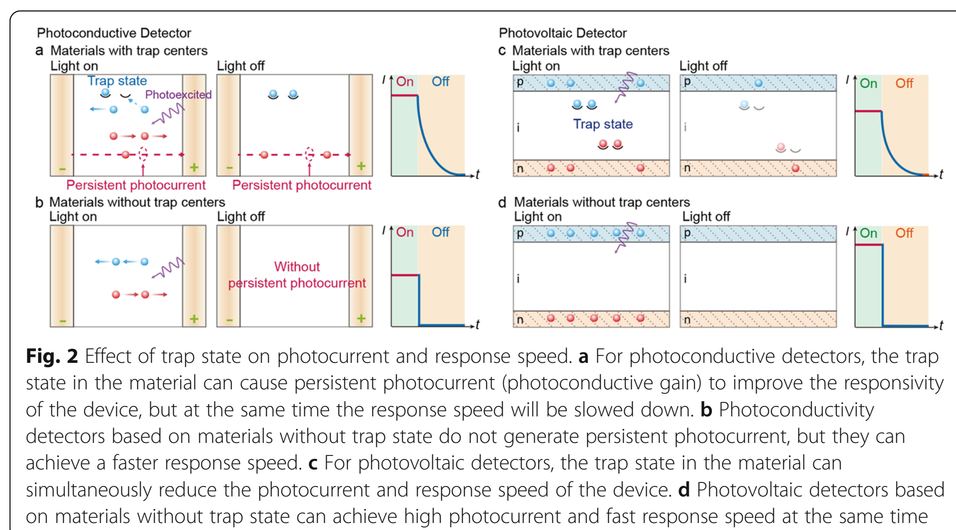

Fig. 2 Effect of trap state on photocurrent and response speed. **a** For photoconductive detectors, the trap state in the material can cause persistent photocurrent (photoconductive gain) to improve the responsivity of the device, but at the same time the response speed will be slowed down. **b** Photoconductivity detectors based on materials without trap state do not generate persistent photocurrent, but they can achieve a faster response speed. **c** For photovoltaic detectors, the trap state in the material can simultaneously reduce the photocurrent and response speed of the device. **d** Photovoltaic detectors based on materials without trap state can achieve high photocurrent and fast response speed at the same time

persistent photoconductive effect caused by excess carriers, so a faster response speed is easier to be achieved.

For photovoltaic detectors, the gain is 1 in general. Thus, in the absence of bias voltage, the photoresponsivity has an upper limit of $R_\lambda = e\lambda/hc$, corresponding to EQE = 100%. Semiconductor depletion region with high electric field, which is used to separate photo-generated electrons from holes, is the most important factor to the performance of photovoltaic detectors. On the one hand, the depletion region must be kept very thin to shorten the transit time; one the other hand, it must be thick enough to absorb most of the incident light. Therefore, in practical application, the thickness of depletion layer must be adjusted appropriately to obtain the optimal quantum efficiency and frequency response. For photovoltaic detectors with a certain structure (with certain width of depletion layer, the detection performance of the device mainly depends on the physical properties of semiconductor materials whose photoresponsivity is negatively correlated with the response time: $R_\lambda \propto f(1/t)$. As illustrated in Fig. 2c, d, the existence of trap states in semiconductors not only reduces the collection efficiency of photo-generated carriers, which leads to a decrease in photoresponsivity, but also increases the response decay time of the device. Thus, it is easier for the photovoltaic detectors based on high-quality semiconductor with low defect density to achieve high responsivity and fast response speed at the same time.

Avalanche gain mechanism

When a large reverse bias voltage is applied to the junction region, the carriers moving in a strong electric field obtain electric field energy and thereby generate new electron-hole pairs through collisional ionization. The newly-generated secondary electrons and holes move to the opposite direction with the influence of electric field, and a new collision ionization can be generated in the movement. A series of collision ionization causes the avalanche multiplication of the number of carriers. Obviously, devices that operate under an avalanche gain mechanism have greater responsivity and are more

suitable for detecting weak optical signals. The multiplication factor is an important parameter used to describe the avalanche effect on the device current amplification factor. In addition, the noise equivalent power is also a key parameter to measure the performance of the avalanche detector. The low noise can be achieved by using two materials with large difference in ionization ability of carriers, that is, carriers with higher ionization ability are injected into the depletion layer. Overall, low-noise and high-gain avalanche detectors have extremely high requirements for the quality of materials and the uniformity of structures.

Performance-test conditions

For the test of the indicators of the photodetector mentioned above, harsh experimental conditions like vacuum environment, VUV light source, special optical components and high-precision electrical instruments are required. One common method to obtain the figure of merit of a photodetector is using a standard synchrotron radiation source (Fig. 3a). Another method is to use a standard detector as the transfer testing standard in the laboratory (Fig. 3b). Typical laboratory VUV light sources include deuterium lamps (continuous spectrum), low-pressure mercury lamps (185 nm), xenon excimer lamps (172 nm), ArF excimer lasers (193 nm) and F_2 excimer lasers (157 nm). Simultaneously, since conventional optical research materials have a strong absorption effect on VUV light, special windows, gratings, filters, etc. are needed, which leaves many physical difficulties and challenges to the performance evaluation of VUV photodetectors.

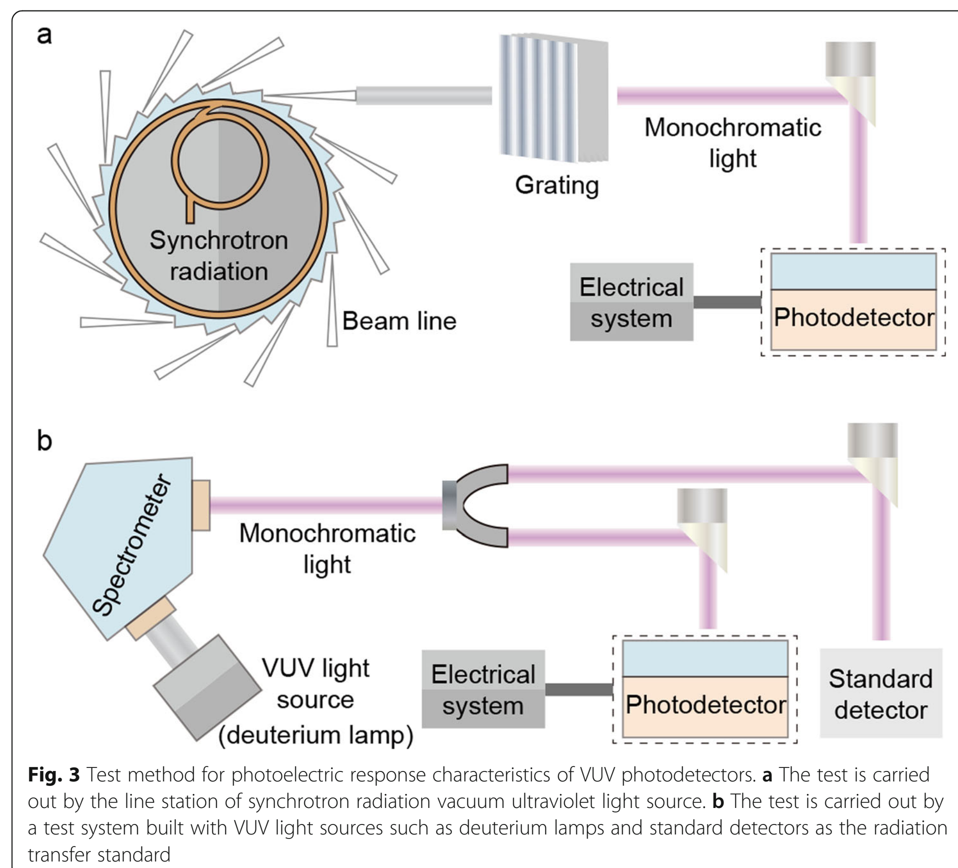

Fig. 3 Test method for photoelectric response characteristics of VUV photodetectors. **a** The test is carried out by the line station of synchrotron radiation vacuum ultraviolet light source. **b** The test is carried out by a test system built with VUV light sources such as deuterium lamps and standard detectors as the radiation transfer standard

Therefore, the development of related technologies for detector testing has also received increasing attention.

VUV-sensitive UWB semiconductors

Diamond with excellent physical properties such as high thermal conductivity, small dielectric constant, and large bandgap energy (~ 5.5 eV, corresponding to the absorption edge of ~ 225 nm) has become an ideal choice for many electronic and optoelectronic applications [30]. In addition, it has been proven to withstand high temperatures, high ionized particle flow as well as intense X-ray and VUV radiation [31–34]. Attempts have been made long before to apply natural or synthetic diamonds to VUV detection technology [35, 36]. However, photodetectors require diamond films to have sufficiently low defect and concentration of n-type and p-type dopants, otherwise the satisfactory detection performance cannot be achieved. Since natural and high-quality diamonds are very expensive and rare, many research teams are committed to exploring how to grow high-quality single crystal diamond films at a low cost [37, 38].

As one of the III-V nitrides materials, cubic BN (c-BN) manifests a series of extreme properties similar to or even better than those of diamond. In sphalerite structure, the atomic density of cubic BN with sp^3 atomic bond is only 4.3% less. Its thermal conductivity is only inferior to diamond, while its oxidation and graphitization temperatures are much higher than those of diamond [39]. More importantly, c-BN's bandgap (~ 6.3 eV) is larger than the diamond's [40, 41], and c-BN can be doped to form n-type and p-type conductivity, which is still difficult for diamond [42, 43]. Unfortunately, the application of c-BN to VUV photodetectors is seriously hampered by the poor quality of available materials (random orientation, limited thickness of films, poor crystallinity and adhesion to substrates caused by non-cubic BN interlayer) [44]. Therefore, similar to the case of diamond, the research on c-BN-based VUV detectors also focuses on how to prepare high-quality film materials [45]. The similarity of structure, properties, technical development and application between diamond and c-BN demonstrates that the synthetic methods of these materials are of mutual referential significance.

As a van der Waals material with excellent long-term stability and electric insulation, two-dimensional (2D) h-BN (E_g = 5.955 eV) with layered structure is an ideal material for VUV detection [46, 47]. In recent years, h-BN has attracted wide attention in the field of vacuum ultraviolet detection due to its low-dimensional conductive channel, high trap state surface density and high photocurrent gain. Current methods available for preparing atomic-scale h-BN nanosheets for VUV detectors include mechanical exfoliation, metal organic chemical vapor deposition, short pulse plasma beam deposition and ion beam sputtering deposition [48–53].

Aluminum nitride (AlN) with ultra-wide direct bandgap (~ 6.2 eV, corresponding to the absorption edge of ~ 200 nm) is another photosensitive material with VUV detection potential among III-V nitrides, which can suppress background noise internally. The high thermal and chemical stability [54] and excellent radiation resistance make it an ideal material for luminescence [55, 56] and VUV detection [57]. Previous studies have shown that AlN epitaxial layers with optical quality comparable to GaN can be

grown on sapphire through metal organic chemical vapor deposition (MOCVD) [58–61], which lays the foundation for the research of detectors based on high quality AlN films.

In addition to the widely-reported semiconductor materials, many other materials with ultra-wide bandgap are also worthy of exploration and further application especially nitrides [62, 63] and oxides. 2D MgO is an example. It has an ultra-wide energy bandgap of about 7.3 eV [64]. In view of that it does not have the same layered structure as h-BN, thus a two-step conformal anneal synthesis method has been proposed to provide a universally applicable way for the growth of other two-dimensional oxides with layered precursors, such as NiO, CaO, CrO, etc. What's more, this is also an effective method to obtain VUV-sensitive materials with specific band gaps through the mixed growth of two different band-gap semiconductors such as MgGaO and MgZnO.

It should be noted that although some UWB semiconductors such as AlGaN, GaN, ZnO, Ga_2O_3 and SiC have also been demonstrated to have the potential for VUV detection, filters are still required in some applications due to bandgap limitations. The semiconductor materials with larger bandgaps (diamond, BN, AlN, etc.) as a focus of this review do not require filtering in practice.

Photoconductive VUV photodetectors

As we all know, the structure of photoconductive detector is usually a semiconductor with two ohmic contacts, which represents a simple and low-cost structural design. In the past decade, considerable progress has been made in the development of photoconductive photodetectors based on these emerging semiconductor materials, and film-structure and nano-structure materials with high quality have been successfully prepared (the quality of materials is the key factor limiting their development).

Film-structure

Chemical vapor deposition (CVD) and high-pressure high-temperature (HPHT) are the two common methods for diamond film growth. In 2005, Z. Remes et al [65] reported the experimental results of photocurrent spectra and instantaneous decay of photocurrent of intrinsic CVD diamond films grown on natural (100) oriented and single-crystal IIA diamond substrates in the same epitaxial manner. The long effective lifetime of photogenerated carriers led to a typical sensitivity that is about 10^{-2} A/W at 200 nm, and a response time less than 0.1 ms. Concurrently, Balducci et al [66] reported the photoresponse characteristics of single-crystal diamond-based VUV detectors by microwave CVD. The photocurrent of the device at 30.4 nm and 58.4 nm proves the photoelectric detection ability of as-fabricated detectors in the extreme ultraviolet spectral region. Moreover, the diamond thin-film detector exhibited long-term stability over 98 h under VUV radiation of 10 mW/cm^2 [67]. Excellent long-term stability is one of the important factors for transfer standard detectors in the VUV band [68].

Metal-semiconductor-metal (MSM) diamond photodetectors have been used in the LYRA [9] of the vacuum ultraviolet solar radiometer. LYRA can provide four ultraviolet bands of solar radiation data with a temporal resolution up to 10 ms, which provides an effective technical support for space solar activity monitoring. In order to evaluate the

usability of photoconductive diamond detectors in lithography, measurements were performed by using various VUV light sources, including low-pressure mercury lamp, xenon excimer lamp, ArF excimer laser and synchrotron radiation (EUV) [11]. The device can detect a 193 nm laser with a pulse width of 5 ns and has a good linear output within a certain energy range. In addition, it is found that the diamond ultraviolet detector has a higher spectral responsivity in the wavelength range of 10-33 nm. These results disclose that diamond detectors have great application potential both for 193 nm and EUV lithography. Since photodetectors are usually packaged in grounded metal vacuum chambers for detection, the photoemission current contributes to the output current. Especially for short-wavelength detection in the VUV range, the photoemission current is not negligible [69]. It is found that in the 10–60 nm wavelength range, the light emission current dominates when the wavelength is greater than 40 nm, while the internal photocurrent plays a major role when the wavelength is less than about 25 nm [70]. In recent years, the development of new device structures mainly focus on improving the light absorption efficiency and carrier transmission efficiency of diamond detectors, including the use of electrodes of different materials, the design of electrodes of different shapes and sizes, and the construction of three-dimensional structures [71–74]. Among them, an all-carbon diamond photodetector achieves the best photoresponsivity of 21.8 A/W (218 nm, 50 V bias) [74].

Nano-structure

Compared with traditional bulk and thin-film structure materials, low-dimensional nanostructured detectors that have a quantum confinement effect on carriers [75–77] are more likely to have higher response rates and faster response speed. Moreover, nano-scale materials have a strong self-exclusion effect of impurities, which makes defects fewer and crystalline quality higher [78].

In order to prepare a VUV photodetector based on low-dimensional AlN, a two-step physical vapor transport method is designed to break the bottleneck of growing defect-free and high-quality micro/nanowires [25]. The method includes a high-temperature process for growing AlN single crystal and a temperature-optimized auxiliary annealing process for reducing defects in nanostructures [79]. Photodetectors based on AlN micro/nanowires are constructed by depositing Au (20 nm) electrodes at an interval of 10 μm onto the micro/nanowires on sapphire substrates, in which the tail of AlN micro/nanowires is covered with indium to improve the physical contact between metal and semiconductor (Inset of Fig. 4a). In addition to the expected low dark current and high breakdown voltage, the spectral response curve indicates that when the energy of incident light exceeds the threshold of 200 nm (6.2 eV), the detector exhibits significant photocurrent gain with a cut-off wavelength of 208 nm (Fig. 4a).

2D materials can efficiently collect photo-generated carriers, which benefits from the low-dimensional conductive channel for fast carrier collection and the high surface state density for photocurrent gain absorption. Typically, VUV photodetectors based on 2D h-BN and MgO with MSM structure are constructed [27, 80] and their VUV detection performance is tested by using synchrotron radiation. The detectors are not

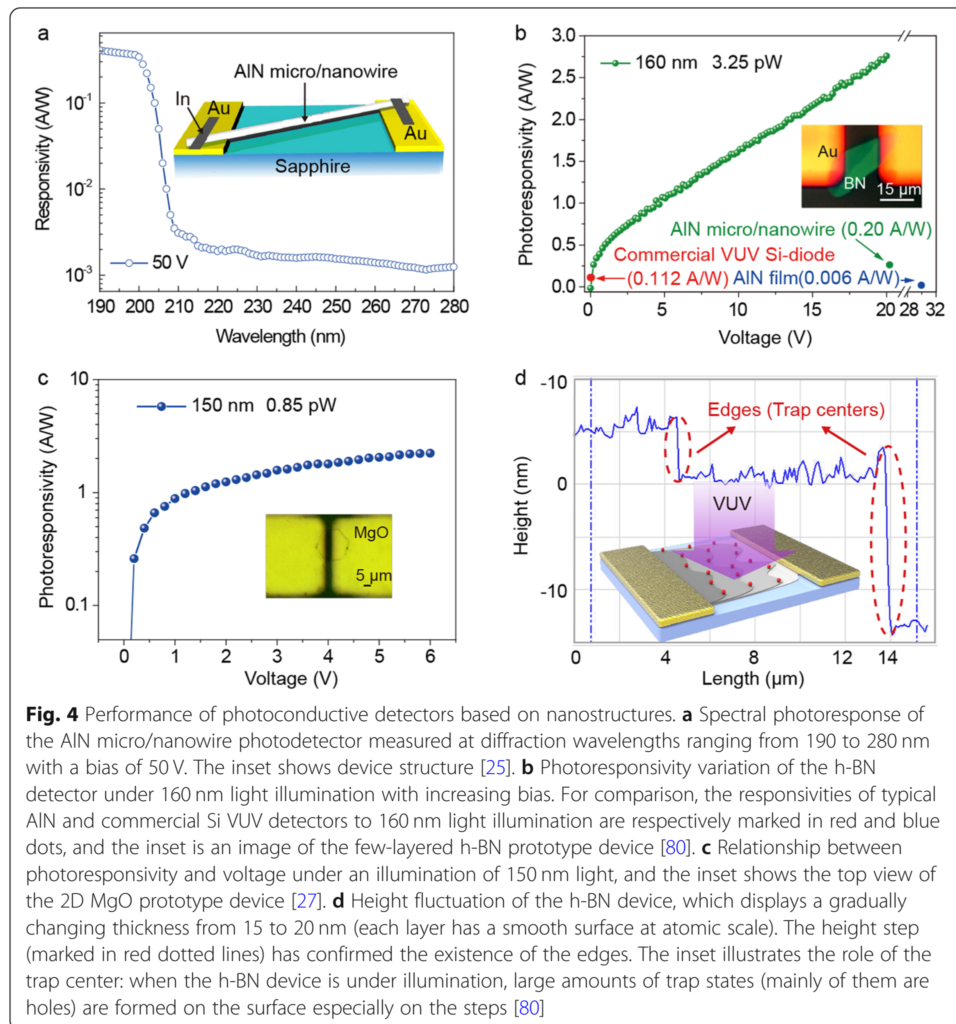

Fig. 4 Performance of photoconductive detectors based on nanostructures. **a** Spectral photoresponse of the AlN micro/nanowire photodetector measured at diffraction wavelengths ranging from 190 to 280 nm with a bias of 50 V. The inset shows device structure [25]. **b** Photoresponsivity variation of the h-BN detector under 160 nm light illumination with increasing bias. For comparison, the responsivities of typical AlN and commercial Si VUV detectors to 160 nm light illumination are respectively marked in red and blue dots, and the inset is an image of the few-layered h-BN prototype device [80]. **c** Relationship between photoresponsivity and voltage under an illumination of 150 nm light, and the inset shows the top view of the 2D MgO prototype device [27]. **d** Height fluctuation of the h-BN device, which displays a gradually changing thickness from 15 to 20 nm (each layer has a smooth surface at atomic scale). The height step (marked in red dotted lines) has confirmed the existence of the edges. The inset illustrates the role of the trap center: when the h-BN device is under illumination, large amounts of trap states (mainly of them are holes) are formed on the surface especially on the steps [80]

only capable of identifying VUV signals of very weak pw power levels, but also achieving external quantum efficiencies up to 2133% and 1539% respectively at certain bias voltages (Fig. 4b, c). This ultra-high photoconductivity gain is mainly due to the contribution of the sustained photoconductivity effect to the photocurrent. The trap centers on the surface of the 2D material to capture the photogenerated carriers and to help form additional electron transport channels (Fig. 4d). Compared with photoconductive detectors based on bulk and film materials, these two two-dimensional materials have been greatly improved when it comes to the response speed (milliseconds).

Although the universal applicability for VUV detection of the photoconductive detectors mentioned above has been proven, further research is necessary on these UWB semiconductors and related technologies to improve the device performance, so as to meet the requirements of practical application in VUV detection. Especially for photoresponse dynamics, methods such as deliberately introducing recombination centers can be implemented to reduce the carrier lifetime and to avoid the nonlinear response.

Photovoltaic VUV photodetectors

Compared with photoconductive VUV detectors, the advantage of photovoltaic VUV detectors exists in the possibility of achieving zero power consumption. Also, because of the built-in electric field used to separate photogenerated carriers, the photovoltaic device can achieve ultra-fast response speed, which is expected to replace the bulky and high-power-consumption conventional VUV detection system in the future.

Single Schottky-barrier photodiodes

For p-doped diamond with boron, the construction of the Schottky structure is feasible. Both planar and vertical configurations can implement Schottky barrier photodiodes. Liao et al. proposed a single Schottky barrier photodiode with interdigitated ohmic contact and Schottky contact (Fig. 5a), which can operate with high gain in photoconductive mode and achieve fast response speed in depletion mode [81]. The homoepitaxial diamond layer was grown on a HPHT synthetic Ib (100) diamond substrate containing typically 100 ppm nitrogen by using a microwave plasma-enhanced CVD technique. Under 220 nm irradiation, the EQE reached 20% at a reverse bias of 30 V and a responsivity more than 18 A/W was obtained at a forward bias of − 23 V. Another vertical structure was constructed by Almaviva et al [82, 84]. Similarly, a conductive boron-doped diamond homoepitaxial layer was grown on a low-cost synthetic HPHT-Ib single crystal diamond substrate by microwave plasma-enhanced CVD and then an intrinsic diamond with a thickness of about 2 μm was uniformly epitaxially grown on the doped layer as a light absorbing layer (PIM structure, Fig. 5b). The diamond detector's responsivity and EQE under two different bias voltages in the 20-80 nm wavelength range are shown in Fig. 5c [82]. The dependence of the device's response on the applied bias voltage varies with the incident wavelength, which may be due to the increase in surface and volume recombination caused by the change in penetration depth. In order to compare the performance of the planar and vertical structure detectors above, the p-type diamond interdigitated electrode was used to construct ohmic contact to control the variables (IDT-PIM structure) [83]. The responsivity of these two different structures varies with wavelength in opposite directions, and it is obvious that the vertical structure is more advantageous in the short wavelength band (Fig. 5d). In addition to the Al electrodes, vertical TiN electrodes have also been used to construct diamond detectors by DC magnetron sputtering and lift-off methods [85]. The detector achieves a responsivity of 0.325 A/W (30 V, 210 nm) and a decay time of ~ 1.2 ms. The EQE of the device exceeds 100% at 60 V bias, which indicates the existence of a certain gain mechanism.

Back-to-back MSM photodiodes

The MSM photovoltaic detector consists of two interdigitated back-to-back diodes, which does not require p-type doping of the semiconductor, and has the advantages like simple structure (planar structure), high sensitivity and easy integration. This structure is often implemented by UWB semiconductor-based detectors for which doping is hard to be achieved.

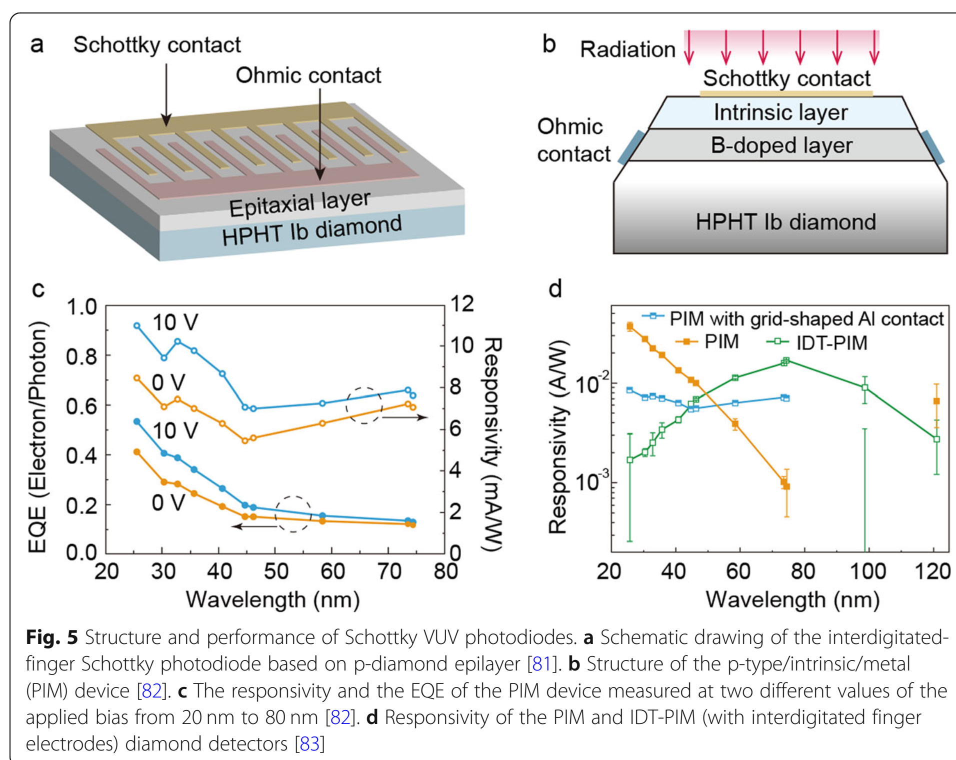

Fig. 5 Structure and performance of Schottky VUV photodiodes. **a** Schematic drawing of the interdigitated-finger Schottky photodiode based on p-diamond epilayer [81]. **b** Structure of the p-type/intrinsic/metal (PIM) device [82]. **c** The responsivity and the EQE of the PIM device measured at two different values of the applied bias from 20 nm to 80 nm [82]. **d** Responsivity of the PIM and IDT-PIM (with interdigitated finger electrodes) diamond detectors [83]

The high surface energy and small atom spacing of c-BN [86] hinder its formation on heterogeneous substrates. Therefore, the selection of substrate materials for depositing c-BN thin films becomes an arduous task of repeated experiments. Some people have tried to grow c-BN on silicon [87], aluminum nitride [88] and diamond [89–91] substrates, among which diamond has been proved to be the optimal substrate for the heteroepitaxial growth of c-BN. Subsequent studies have shown that diamond can be deposited as a general intermediate layer on a variety of materials with good adhesion and crystallinity to form composite structures for the growth of pure (i.e. not in the form of non-cubic BN) and adhesive c-BN films on all these materials [92–94]. It has been reported that with the help of He-Ar-N_2-BF_3-H_2 gas mixture, a VUV photodetector based on c-BN films was fabricated by depositing c-BN films on diamond-coated silicon substrates in an electron cyclotron resonance microwave plasma CVD system (Fig. 6a) [95]. The collimating and tunable monochromatic beams were used to measure the spectral response of a c-BN-based photodetector and the spectral responsivity curve was plotted by using AXUV silicon photodiode for calibration. It can be observed from Fig. 6b that under the bias voltages of – 20, – 30 and -35 V, the maximum response at about 180 nm is 12, 23 and 32 mA/W respectively. At about 193 nm, the device has a very sharp cut-off wavelength corresponding to the bulk c-BN bandgap. The measured rejection ratio (the ratio of responsivity between 180 and 250 nm) exceeds four orders of magnitude, suggesting that c-BN-based detectors are able to directly detect VUV radiation and eliminate any mid-ultraviolet noise.

For AlN with difficult p-type doping, the back-to-back MSM structure is a comprehensive optimal choice. Researchers demonstrate the development and utilization of high-quality AlN thin films in VUV photodetectors, and their outstanding

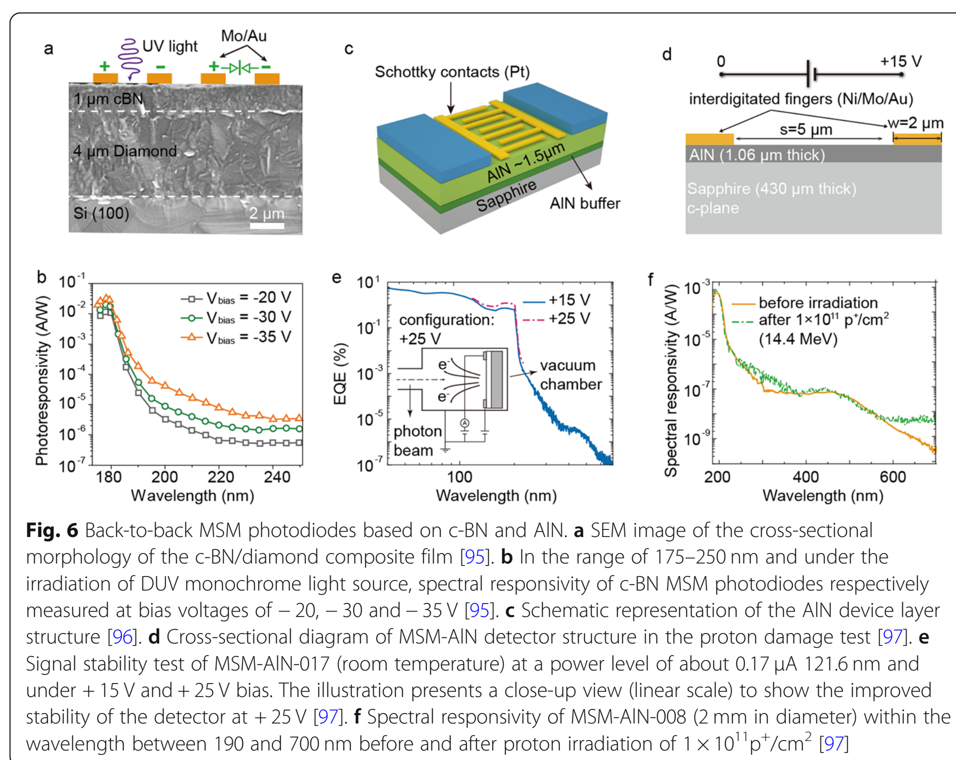

Fig. 6 Back-to-back MSM photodiodes based on c-BN and AlN. **a** SEM image of the cross-sectional morphology of the c-BN/diamond composite film [95]. **b** In the range of 175–250 nm and under the irradiation of DUV monochrome light source, spectral responsivity of c-BN MSM photodiodes respectively measured at bias voltages of – 20, – 30 and – 35 V [95]. **c** Schematic representation of the AlN device layer structure [96]. **d** Cross-sectional diagram of MSM-AlN detector structure in the proton damage test [97]. **e** Signal stability test of MSM-AlN-017 (room temperature) at a power level of about 0.17 μA 121.6 nm and under + 15 V and + 25 V bias. The illustration presents a close-up view (linear scale) to show the improved stability of the detector at + 25 V [97]. **f** Spectral responsivity of MSM-AlN-008 (2 mm in diameter) within the wavelength between 190 and 700 nm before and after proton irradiation of $1 \times 10^{11} p^+/cm^2$ [97]

characteristics are reported [96]. Figure 6c shows a schematic diagram of the device layer structure used in this study, which adopts an undoped 1.5-um-thick AlN epitaxial layer as the active layer. The device presents extremely low dark current of about 100 fA at a bias voltage of 200 V (system limitation). The peak response of 200 nm, pretty sharp cut-off wavelength of 207 nm, and VUV to UV/visible light rejection ratio of more than four orders of magnitude all indicate that AlN-based photodetectors are promising in the application of VUV detection. Later, Tsai et al. fabricated a MSM photodetector by deposing the AlN film on Si (100) substrates, which showed high temperature resistance and radiation tolerance for harsh environments [98].

It is well-known that high-density threading dislocations (TDs) and inverted domains (IDs) with N polarity significantly reduce the performance of III nitride-based devices. Pantha et al have observed a strong correlation between the dark current and sensitivity of MSM photodetectors in MOCVD AlN and the TD density [99]. In order to investigate the effect of ID on the photoelectric properties of AlN-based MSM photodetectors, Large-area MSM photodetectors based on AlN layers with different densities of IDs have been fabricated, and the effects of ammonia molecular beam epitaxy growth conditions on the structure and morphology of AlN have been studied [100]. The results show that the smallest root-mean-square (rms) roughness and the optimal crystal integrity are generated by nitriding at high ammonia flow rate. Subsequent TEM measurements verify that the ID originates from the sapphire/AlN interface. After the growth of nucleating layers of AlN, two AlN/GaN short-period super-lattices are introduced to significantly reduce the ID density by an order of magnitude, while the TD density is basically unchanged. Both low-density and high-density ID samples are used to fabricate MSM photodetectors. Athough the device with ID density of 10^6 cm^{-2} (low density) has a performance comparable to that with AlN grown by MOCVD, its

responsivity is very poor. This is because illumination or photo-degradation will result in a decrease of photocurrent, which can be attributed to the formation of metastable defects of positioning carriers [101–103].

Similar to diamond, the well-known parasitic phenomenon is that when the photo-generated electrons have enough energy, they will emanate photoemission from the device. In order to verify the applicability of AlN-based MSM photodetectors for VUV detection, Ben Moussa et al [104] studied the influence of photoemission current on output signals. At the PTB-Bessy II Synchrotron Radiation Beam (B), the AlN MSM photodiode is mounted in the operating stage bracket. It is concluded that the whole circuit is biased to the energy higher than the maximum kinetic energy (e.g. dozens of electron volts) that can be obtained after electrons leave the surface. In other words, the AlN MSM detector is operated at positively high bias voltages to maximize output signals and to reduce the escape probability of electrons, which thus proves that photodetectors based on wide band-gap semiconductors have the advantages of high rejection ratio and high output signal in VUV solar observations. For practical application, the optical components of detectors are usually directly exposed to solar radiation, so ionization and atomic displacement damage effects are the main reasons for the degradation of space instruments. In order to explore their effects, the same research group [97] manufactured a large-area AlN circular MSM detector with diameter of 1.1–4.3 mm by using an interdigital electrode with a width of 2 μm and a spacing of 5 μm (Fig. 6d), and it was mounted in a ceramic package with a removable glass protective device. The spectral responsivity and irradiation stability of the device in the wavelength range of 40–700 nm are measured. As shown in Fig. 6e, the detector exhibits a high rejection ratio of about five orders of magnitude between 200 nm and 450 nm, which meets the strict requirement for unfiltered VUV solar observations. After the exposure to protons with 14.4 MeV energy, no significant reduction in detector performance is observed (Fig. 6f), which shows good radiation tolerance and further proves the universal feasibility of AlN MSM detectors for space application.

Heterojunction photovoltaic photodetectors

The selection and optimization of the functional layer is the key to the preparation of heterojunction photovoltaic vacuum ultraviolet detectors, which is involved in energy band engineering. Typically, several PIN diamond photodiodes of circular shape have been fabricated for the solar mission LYRA [105, 106]. The p-type and n-type doping of diamond was achieved by boron and phosphorus, respectively, and a thin Al layer ($<$ 10 nm) with a transmittance of typically 20% to 50% was deposited for the top contact. The responsivity of the detector is 27.2 mA/W at 200 nm, displaying a UV/visible ratio (200 nm/500 nm) of six orders of magnitude. In the wavelength range of interest, PIN photodiodes are reasonably homogeneous, linear and stable under brief irradiation, which have the potential to meet the requirements of LYRA.

For UWB semiconductors as photosensitive layers, it is difficult to obtain an optimal upper window layer (conductive transmission layer) that is transparent to VUV light. Although the VUV transmittance can be improved by reducing the

thickness of the metal electrode, the transmittance of even a thin layer (≤10 nm) is not large enough. Graphene (Gr) is widely used as electrode material because of its high mobility. Recently, Gr has been revealed to have a transmittance up to 96% by ultraviolet spectrum transmission experiments [107] in the VUV band due to its weak resistance to electromagnetic waves [108] (Fig. 7a). Therefore, graphene is an excellent candidate for the conductive window layer of VUV photovoltaic detectors.

The construction of a heterojunction photovoltaic device (Fig. 7b) with a PN characteristic vertical structure by using p-type graphene as a transparent electrode to collect carriers confirms the availability of graphene studied by Zheng et al. [107] With the back-to-back heterojunction structure of p-Gr/AlN/p-GaN, the thermal diffusion of carriers is effectively suppressed [109], resulting in a lower noise voltage density, which contributes to the detection of ultra-weak VUV signals. Under the irradiation of 185 nm monochromatic light (from the characteristic spectral line of low-voltage mercury lamp), an electromotive force of 1.7 V will be formed at both ends of the device and a stable open-circuit voltage can be output, but in dark state and under 250 nm light no response is seen (Fig. 7c). A thick space charge region is formed in the heterojunction composed of high-carrier-concentration p-Gr and low-carrier-concentration i-AlN. When VUV photons penetrate graphene into the absorption layer of AlN, most of them are absorbed in the space charge region near the p-Gr side of AlN to produce photo-generated electron-hole pairs. Then, electrons and holes are separated by the built-in electric

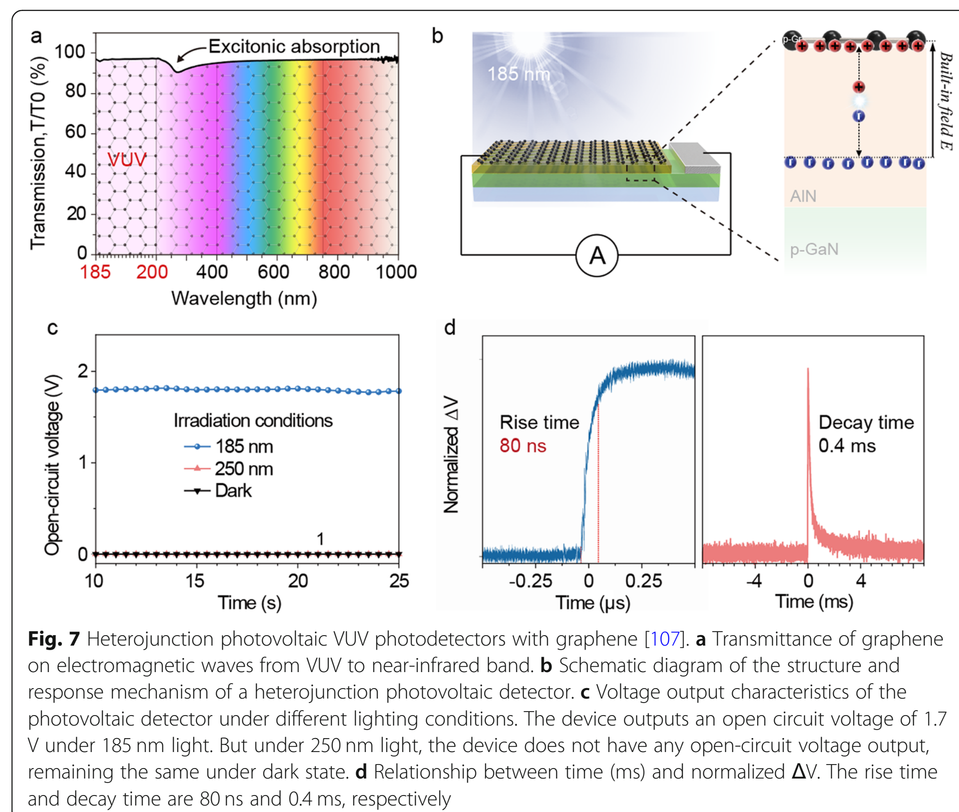

Fig. 7 Heterojunction photovoltaic VUV photodetectors with graphene [107]. **a** Transmittance of graphene on electromagnetic waves from VUV to near-infrared band. **b** Schematic diagram of the structure and response mechanism of a heterojunction photovoltaic detector. **c** Voltage output characteristics of the photovoltaic detector under different lighting conditions. The device outputs an open circuit voltage of 1.7 V under 185 nm light. But under 250 nm light, the device does not have any open-circuit voltage output, remaining the same under dark state. **d** Relationship between time (ms) and normalized ΔV. The rise time and decay time are 80 ns and 0.4 ms, respectively

field: the holes drift to the p-Gr side, while the electrons drift to the opposite direction, resulting in an open-circuit voltage of 1.7 V. Time response test is conducted by using 193 nm nanosecond pulses to simulate ultra-fast changing VUV signal sources, showing that the device has an encouraging ultra-fast rise time of only 80 ns (Fig. 7d) which is 10^4–10^6 times faster than that of the VUV detectors reported currently.

Drawing on the work above, VUV detectors based on other UWB photosensitive materials are also introduced. As we know, the band gap can be controlled by adjusting the composition of the compound. For example, the compound with a band gap between 4.8–7.3 eV can be obtained by the mixed growth of MgO and Ga_2O_3. Amorphous MgGaO (~ 6.0 eV) is grown on n-type GaN [110] and n-type SiC [111] substrates respectively, and the responsivity of 2 mA/W and 10 mA/W (under 185 nm radiation) are obtained by using graphene as window layer. In addition, graphene has also been used to construct diamond heterojunction detectors [112]. The research results above prove the universality of using graphene to construct heterojunction VUV detectors, and provide a new scheme for the development of integrated VUV photodetectors with zero power consumption, ultra-high speed and high sensitivity.

Improvement of photovoltaic performance

We have noticed that in the impulse response experimental results of the above studies, the decay time of the device at room temperature is still much longer than the ultrafast rise time of photoresponse. In order to explore the response time mechanism of the device for the reduction in decay time, a p-Gr/AlN/n-ZnO heterojunction photovoltaic detector with PIN characteristics is constructed [113]. According to the previous description, the rise time of photodetectors mainly depends on the transit time of the uncaptured photo-generated carriers drifting to the electrodes, while the exponential response attenuation mainly results from the capture of photo-generated carriers by internal defects and/or surface states, that is, the lifetime of so-called trap states directly determines the decay time of photoresponse. Therefore, it is theoretically possible to use external heating to provide active energy for trap carrier escape and accelerate the annihilation of trap states, and then the carriers can be quickly collected instead of being captured by trap centers to reduce decay time. Temperature-dependent time response tests (Fig. 8a) confirm the effectiveness of the proposed strategy. With the increase of temperature, the photocurrent of the device gradually increases, while the decay time of the device decreases rapidly (Fig. 8b). Furthermore, the proposed instantaneous response mechanism of thermally-enhanced wide-bandgap semiconductor-based photovoltaic devices is universally applicable.

As we all know, for photovoltaic detectors, increasing the open-circuit voltage of the device is useful to obtain a larger voltage signal output and higher external quantum efficiency [116, 117]. For vertical structure heterojunction detectors, efficient energy band assembly is the key method to increase the potential difference across the device and then to increase the open-circuit voltage [118]. The optimized device structure is designed through comparison of different electrode materials by Jia et al., and an open-

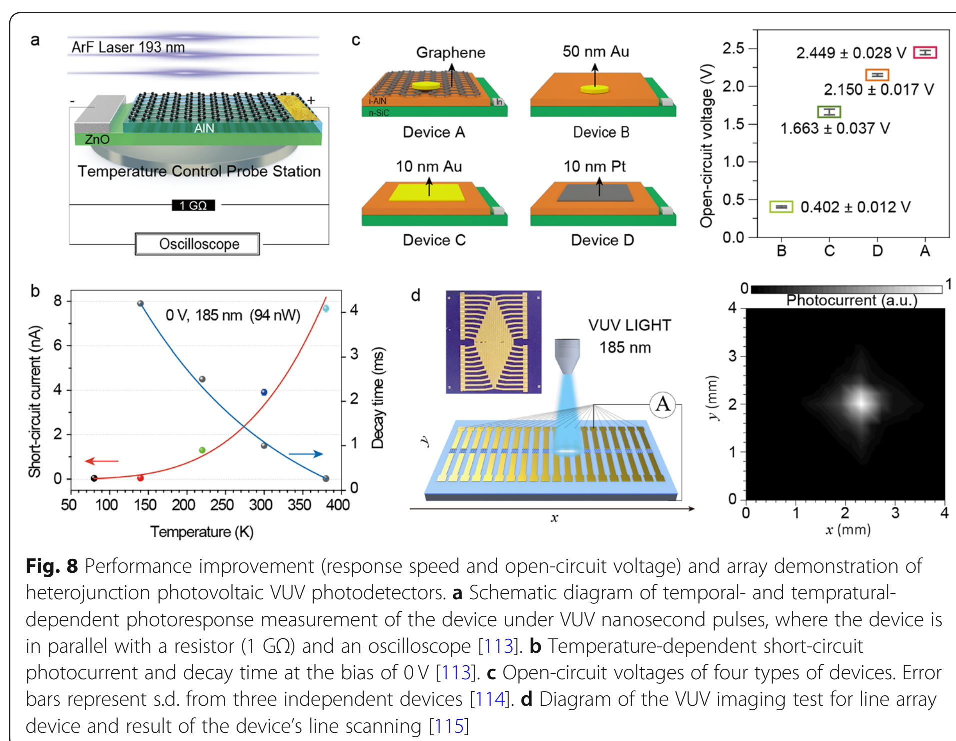

Fig. 8 Performance improvement (response speed and open-circuit voltage) and array demonstration of heterojunction photovoltaic VUV photodetectors. **a** Schematic diagram of temporal- and temprataral-dependent photoresponse measurement of the device under VUV nanosecond pulses, where the device is in parallel with a resistor (1 GΩ) and an oscilloscope [113]. **b** Temperature-dependent short-circuit photocurrent and decay time at the bias of 0 V [113]. **c** Open-circuit voltages of four types of devices. Error bars represent s.d. from three independent devices [114]. **d** Diagram of the VUV imaging test for line array device and result of the device's line scanning [115]

circuit voltage of up to 2.45 V was realized for the first time (Fig. 8c) [114]. Under irradiation, the holes generated by the AlN absorption layer are injected into the graphene, so that the density of the hole state of the graphene increases significantly, resulting in the Fermi level's being lowered. Predictably, this detector exhibits high EQE (56.1%) and fast response speed (rise time≈45 ns). This work clarifies the various possibilities brought by the unique properties of graphene to improve the performance of the device through the effective comparison experiment of control variables for the first time.

Obviously, one of the significant advantages of semiconductor detectors is their ease of integration, which is also the ultimate development trend of UWB semiconductor-based VUV detectors for a wide range of applications. For example, the most intuitive way to monitor solar storms is to use VUV detectors for imaging [119]. In order to realize VUV imaging, ultra-fast response speed is the primary requirement. Moreover, the array structure of detectors is also needed. AlN-based VUV detectors have been demonstrated in the aspect of their integrability: Twenty p-Gr / AlN / p-Si composite heterostructure arrays are fabricated on silicon wafers (the size of each unit is 200 μm × 5 μm) [115]. The circular VUV spots of a certain diameter are obtained through the focus of quartz objective lens for imaging test. When the y-axis is fixed, a linear image can be obtained first. Later, with the movement of the device along the y-axis, the final VUV image can be obtained by the detection of interline currents (Fig. 8d). The excellent detection performance of the device unit is a prerequisite for obtaining the expected imaging, and further research on the large-area process technology still requires researchers' great efforts.

Avalanche VUV photodetectors

Broadly speaking, avalanche detector also belongs to a photovoltaic detector according to its structure. However, since its working mode and mechanism are special, it is discussed separately here. Avalanche photodetectors have the advantages of high sensitivity, fast speed and high optical gain. The reverse bias applied to the junction is close to the breakdown voltage to stimulate the avalanche effect. Because the realization of avalanche VUV detectors has high requirements for the quality of UWB materials and construction processes, and it is limited by cost and technical difficulties, thus there is still few researches in this field. Nonetheless, the application potential of UWB semiconductor-based avalanche VUV detectors in many cutting-edge technologies such as single photon detection should still be valued.

Avalanche multiplication effect in diamond

High breakdown voltage or field is considered as a major advantage of diamond. So far, the charge multiplication effect has been observed in intrinsic, p-type and n-type doped CVD diamond structures [120–122]. Due to the difference in doping concentration and device structure or insufficient design, the data reported in various literature are different. Among them, the result of a high breakdown field of 20 MV/cm is relatively reliable and reproducible. Atsushi Hiraiwa et al. established a method to extract the ionization coefficient from the arbitrary relationship between breakdown voltage and doping density and developed a method to simplify the ionization integration [123]. It is found that the breakdown field of diamond is more dependent on the doping density than other materials. Although the enhanced activation of impurities at high temperature significantly improves the performance of diamond, the problem of thermal runaway still needs attention. An accurate understanding of these physical processes is essential to the design and application of high-performance detectors. At present, the application demonstration of diamond-based avalanche detectors is mostly in the field of particle detection. More evaluation on the VUV detection performance of diamond-based avalanche detectors are still in demand.

AlN avalanche photodetectors

The growth of high-quality crystals and the lattice matching of different functional layers are the prerequisites for achieving low-noise and high-gain detectors. The high-quality AlN and SiC interface and good lattice matching (the mismatch rate is 1%) [124, 125], as well as the presence of a conductive SiC substrate, provide feasibility for the preparation of AlN / n-SiC vertical avalanche detectors. An avalanche detector based on AlN / n-SiC Schottky diode structure has been reported [126, 127], and its schematic diagram is shown in Fig. 9a. Schottky contact area is defined by evaporating a 6 nm thick Pt layer followed by photolithography and lift-off. The peak response wavelength and cut-off wavelength are 200 nm and 210 nm, respectively. At a reverse bias of − 250 V ($E_b = 2.8$ MV/cm), a photocurrent gain of 1200 is achieved (Fig. 9b) [127]. In order to realize the device working in Geiger mode, further researches on reducing the dislocation density, optimizing the device size and geometric structure still need to be carried out.

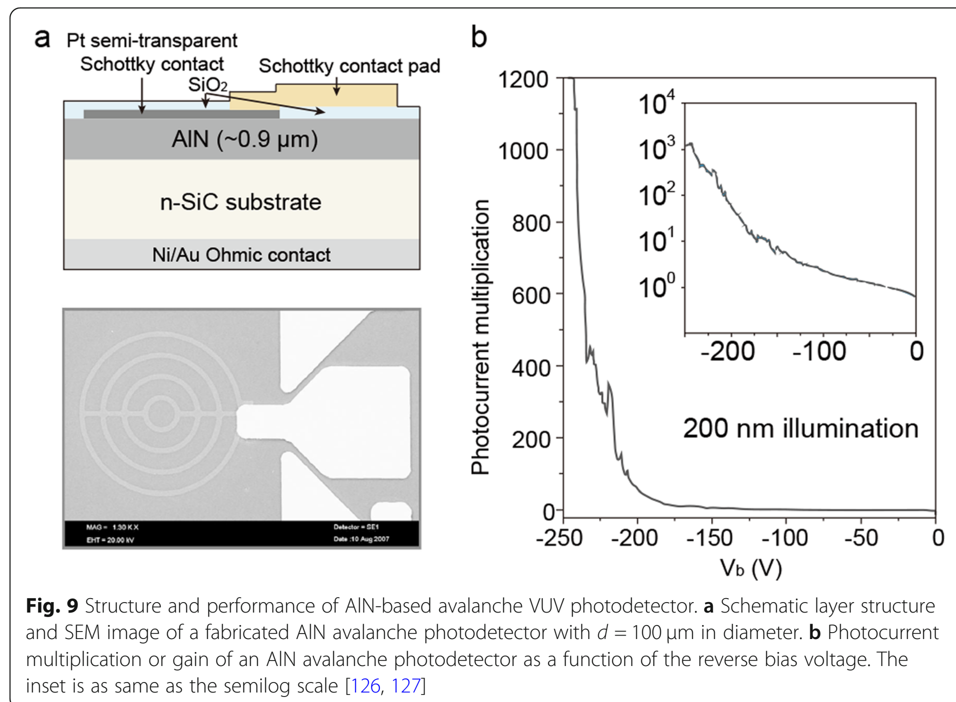

Fig. 9 Structure and performance of AlN-based avalanche VUV photodetector. **a** Schematic layer structure and SEM image of a fabricated AlN avalanche photodetector with $d = 100\,\mu m$ in diameter. **b** Photocurrent multiplication or gain of an AlN avalanche photodetector as a function of the reverse bias voltage. The inset is as same as the semilog scale [126, 127]

Conclusions

Photosensitive materials such as diamond, c-BN, AlN, etc. with the advantages of high radiation hardness, low dark current, high chemical stability and room temperature thermal stability have great application prospects in vacuum ultraviolet detection. Researches on photodetectors based on these emerging semiconductor materials have made considerable progress. The film-structure VUV detector may move faster towards practical productization due to its high stability with more integration process achieved. Future work should still focus on the growth of high-quality thin films, the free control of carriers, and the design of optimized integrated structures. Although emerging nanostructured devices have unique advantages in terms of VUV detection performance, their stability and integration technology still wait for a breakthrough. In addition, the development of new UWB semiconductor materials (in different dimensions) also brings more possibilities for VUV photodetectors.

The general characteristics of these photodetectors and the EQE of some representative results have been summarized in Fig. 10. For different applications' needs, a reasonable trade-off between high quantum efficiency and high frequency response is necessary. For example, in space exploration, it is usually required to minimize the power consumption and response time because the former one is often the most direct and effective way to reduce equipment costs. Meanwhile, in order to monitor solar activity in real time, ultra-fast response time is also indispensable. Therefore, heterojunction photovoltaic detectors with ultra-fast response speed are the best choice in this field.

In the future, researchers should devote their work to the development of imaging technology of flat panel detectors. It has long been expected by scientists to take pictures of ultra-fast dynamic processes in celestial activities, such as recording the early

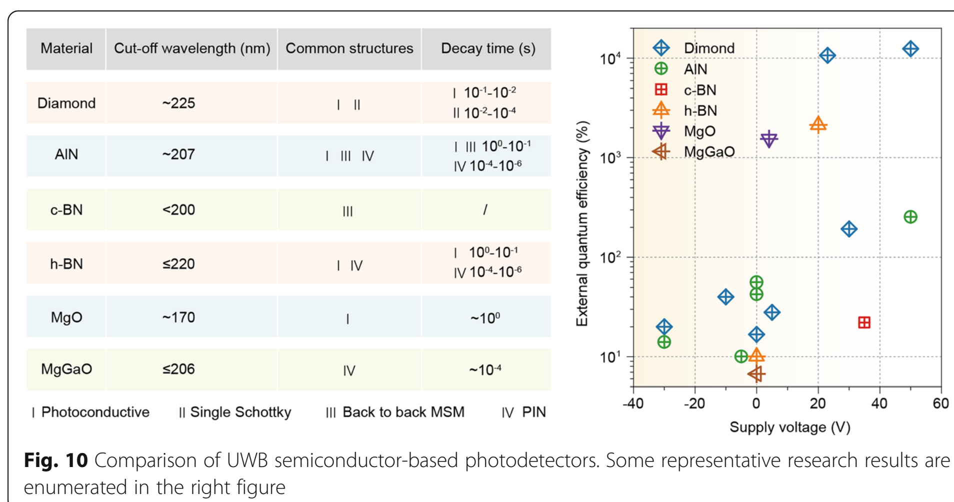

Material	Cut-off wavelength (nm)	Common structures	Decay time (s)
Diamond	~225	I II	I 10^{-1}-10^{-2} II 10^{-2}-10^{-4}
AlN	~207	I III IV	I III 10^{0}-10^{-1} IV 10^{-4}-10^{-6}
c-BN	<200	III	/
h-BN	≤220	I IV	I 10^{0}-10^{-1} IV 10^{-4}-10^{-6}
MgO	~170	I	~10^{0}
MgGaO	≤206	IV	~10^{-4}

I Photoconductive II Single Schottky III Back to back MSM IV PIN

Fig. 10 Comparison of UWB semiconductor-based photodetectors. Some representative research results are enumerated in the right figure

evolution of the original orbit and detecting the chemical composition of coronal jets in solar storms. Especially, achieving single photon detection is also the ultimate goal of VUV photodetectors. At present, only few studies have reported the avalanche detectors based on UWB semiconductors, and the research on single-photon detection performance is still blank. Accordingly, the development of related technologies for detection performance evaluation also needs to be further promoted. The characteristics currently exhibited by UWB semiconductor-based VUV photodetectors shed light on their huge application potential in the frontier field, and related research still has a long way to go.

Abbreviations

VUV: Vacuum-ultraviolet; EUV: Extreme ultraviolet; FEL: Free-electron lasers; UWB: Ultra-wide bandgap; LYRA: Large Yield Radiometer; EQE: External quantum efficiency; CVD: Chemical vapor deposition; HPHT: High-pressure high-temperature; MSM: Metal-semiconductor-metal; Gr: Graphene

Acknowledgements

Not applicable.

Authors' contributions

Wei Zheng and Feng Huang provided an outline and guided writing. Lemin Jia wrote the manuscript and prepared the figures. The author(s) read and approved the final manuscript.

Funding

This work is supported by the National Natural Science Foundation of China (NSFC) (61427901, 61604178, 91333207, U1505252).

Availability of data and materials

Data sharing is not applicable to this article as no new data were created or analysed in this study.

Competing interests

The authors declare that they have no competing interests.

Received: 3 August 2020 Accepted: 25 October 2020
Published online: 09 November 2020

References

1. de Oliveira N, Joyeux D, Nahon L. Spectroscopy in the vacuum-ultraviolet. Nat Photonics. 2011;5:249.
2. Pile DFP. Vacuum-ultraviolet source. Nat Photonics. 2018;12(10):568.
3. Baker D, Kanekal S, Li X, Monk S, Goldstein J, Burch J. An extreme distortion of the Van Allen belt arising from the 'Hallowe'en'solar storm in 2003. Nature. 2004;432(7019):878.
4. Guerrero MA, De Marco O. Analysis of far-UV data of central stars of planetary nebulae: Occurrence and variability of stellar winds. Astronomy Astrophysics. 2013;553:A126.

5. Gosling JT, Asbridge JR, Bame SJ, Feldman WC. Solar wind stream interfaces. J Geophys Res Space Physics. 1978;83(A4):1401–12.
6. Cane HV, Richardson IG. Interplanetary coronal mass ejections in the near-Earth solar wind during 1996–2002. J Geophysical Res Space Physics. 2003;108(A4):1156. https://doi.org/10.1029/2002JA009817.
7. Sibeck DG, Lopez RE, Roelof EC. Solar wind control of the magnetopause shape, location, and motion. J Geophys Res Space Physics. 1991;96(A4):5489–95.
8. Shea MA, Smart DF, McCracken KG, Dreschhoff GAM, Spence HE. Solar proton events for 450 years: the Carrington event in perspective. Adv Space Res. 2006;38(2):232–8.
9. BenMoussa A, Dammasch IE, Hochedez J-F, Schühle U, Koller S, Stockman Y, et al. Pre-flight calibration of LYRA, the solar VUV radiometer on board PROBA2. Astron Astrophys. 2009;508(2):1085–94.
10. Torr M, Torr D, Zukic M, Johnson R, Ajello J, Banks P, et al. A far ultraviolet imager for the international solar-terrestrial physics mission. Space Sci Rev. 1995;71(1–4):329–83.
11. Ishihara H, Sugio S, Kanno T, Matsuoka M, Hayashi KJS. Characterization of Photoconductive Diamond Detectors--Candidate Vacuum Ultraviolet Radiation and Extreme Ultraviolet Radiation Light Source Detectors for Lithography. Sensors Mater. 2010;22(7):357–64.
12. Antonelli M, Di Fraia M, Carrato S, Cautero G, Menk RH, Jark WH, et al. Fast synchrotron and FEL beam monitors based on single-crystal diamond detectors and InGaAs/InAlAs quantum well devices. Nucl Instrum Methods Phys Res Section A: Accelerators, Spectrometers, Detectors Assoc Equip. 2013;730:164–7.
13. Venot O, Fray N, Bénilan Y, Gazeau M-C, Hébrard E, Larcher G, et al. High-temperature measurements of VUV-absorption cross sections of CO2 and their application to exoplanets. A&A. 2013;551:A131.
14. Moos HW, Cash WC, Cowie LL, Davidsen AF, Dupree AK, Feldman PD, et al. Overview of the far ultraviolet spectroscopic explorer Mission. Astrophys J Lett. 2000;538(1):L1.
15. BenMoussa A, Soltani A, Schühle U, Haenen K, Chong YM, Zhang WJ, et al. Recent developments of wide-bandgap semiconductor based UV sensors. Diam Relat Mater. 2009;18(5):860–4.
16. BenMoussa A, Hochedez JF, Schühle U, Schmutz W, Haenen K, Stockman Y, et al. Diamond detectors for LYRA, the solar VUV radiometer on board PROBA2. Diam Relat Mater. 2006;15(4):802–6.
17. McComas DJ, Christian ER, Cohen CMS, Cummings AC, Davis AJ, Desai MI, et al. Probing the energetic particle environment near the Sun. Nature. 2019;576(7786):223–7.
18. Kasper JC, Bale SD, Belcher JW, Berthomier M, Case AW, Chandran BDG, et al. Alfvénic velocity spikes and rotational flows in the near-Sun solar wind. Nature. 2019;576(7786):228–31.
19. Howard RA, Vourlidas A, Bothmer V, Colaninno RC, DeForest CE, Gallagher B, et al. Near-Sun observations of an F-corona decrease and K-corona fine structure. Nature. 2019;576(7786):232–6.
20. Bale SD, Badman ST, Bonnell JW, Bowen TA, Burgess D, Case AW, et al. Highly structured slow solar wind emerging from an equatorial coronal hole. Nature. 2019;576(7786):237–42.
21. Hansen TE. Silicon UV-photodiodes using natural inversion layers. Phys Scr. 1978;18(6):471.
22. Korde R, Geist J. Quantum efficiency stability of silicon photodiodes. Appl Opt. 1987;26(24):5284–90.
23. Korde R, Geist J. Stable, high quantum efficiency, UV-enhanced silicon photodiodes by arsenic diffusion. Solid·State Electron. 1987;30(1):89–92.
24. Shizuo F. Wide-bandgap semiconductor materials: for their full bloom. Jpn J Appl Phys. 2015;54(3):030101.
25. Zheng W, Huang F, Zheng R, Wu H. Low-dimensional structure vacuum-ultraviolet-sensitive (λ < 200 nm) Photodetector with fast-response speed based on high-quality AlN micro/nanowire. Adv Mater. 2015;27(26):3921–7.
26. Zheng W, Jia L, Huang F. Vacuum-Ultraviolet Photon Detections. iScience. 2020;23(6):101145.
27. Zheng W, Lin R, Zhu Y, Zhang Z, Ji X, Huang F. Vacuum ultraviolet Photodetection in two-dimensional oxides. ACS Appl Mater Interfaces. 2018;10(24):20696–702.
28. Sukhovatkin V, Hinds S, Brzozowski L, Sargent EH. Colloidal quantum-dot Photodetectors exploiting Multiexciton generation. Science. 2009;324(5934):1542–4.
29. Zheng W, Xiong X, Lin R, Zhang Z, Xu C, Huang F. Balanced Photodetection in one-step liquid-phase-synthesized CsPbBr3 micro−/Nanoflake single crystals. ACS Appl Mater Interfaces. 2018;10(2):1865–70.
30. Pace E, Di Benedetto R, Scuderi S. Fast stable visible-blind and highly sensitive CVD diamond UV photodetectors for laboratory and space applications. Diam Relat Mater. 2000;9(3):987–93.
31. Alison M. Recent developments of diamond detectors for particles and UV radiation. Semicond Sci Technol. 2000;15(9):R55.
32. Fahrner WR, Job R, Werner M. Sensors and smart electronics in harsh environment applications. Microsyst Technol. 2001;7(4):138–44.
33. Monroy E, Omnès F, Calle F. Wide-bandgap semiconductor ultraviolet photodetectors. Semicond Sci Technol. 2003;18(4):R33.
34. Hochedez JF, Verwichte E, Bergonzo P, Guizard B, Mer C, Tromson D, et al. Future Diamond UV Imagers For Solar Physics. Physica Status Solidi (a). 2000;181(1):141–9.
35. McKeag RD, Jackman RB. Diamond UV photodetectors: sensitivity and speed for visible blind applications. Diam Relat Mater. 1998;7(2):513–8.
36. Barberini L, Cadeddu S, Caria M. A new material for imaging in the UV: CVD diamond. Nucl Instrum Methods Physics Res Section A: Accelerators, Spectrometers, Detectors Assoc Equipment. 2001;460(1):127–37.
37. Teraji T, Yoshizaki S, Wada H, Hamada M, Ito T. Highly sensitive UV photodetectors fabricated using high-quality single-crystalline CVD diamond films. Diam Relat Mater. 2004;13(4):858–62.
38. Kaneko JH, Teraji T, Hirai Y, Shiraishi M, Kawamura S, Yoshizaki S, et al. Response function measurement of layered type CVD single crystal diamond radiation detectors for 14 MeV neutrons. Rev Sci Instrum. 2004;75(10):3581–4.
39. Solozhenko VL, Turkevich VZ, Holzapfel WB. Refined phase diagram of boron nitride. J Phys Chem B. 1999;103(15):2903–5.
40. Miyata N, Moriki K, Mishima O, Fujisawa M, Hattori T. Optical constants of cubic boron nitride. Phys Rev B. 1989;40(17):12028–9.
41. Spear KE. Diamond—ceramic coating of the future. J Am Ceram Soc. 1989;72(2):171–91.

42. Noor Mohammad S. Electrical characteristics of thin film cubic boron nitride. Solid-State Electron. 2002;46(2):203–22.
43. Kalish R. Doping of diamond. Carbon. 1999;37(5):781–5.
44. Zhang WJ, Chong YM, Bello I, Lee ST. Nucleation, growth and characterization of cubic boron nitride (cBN) films. J Phys D Appl Phys. 2007;40(20):6159.
45. Samantaray CB, Singh RN. Review of synthesis and properties of cubic boron nitride (c-BN) thin films. Int Mater Rev. 2005;50(6):313–44.
46. Watanabe K, Taniguchi T, Niiyama T, Miya K, Taniguchi M. Far-ultraviolet plane-emission handheld device based on hexagonal boron nitride. Nat Photonics. 2009;3:591.
47. Cassabois G, Valvin P, Gil B. Hexagonal boron nitride is an indirect bandgap semiconductor. Nat Photonics. 2016;10:262.
48. Sajjad M, Jadwisienczak WM, Feng P. Nanoscale structure study of boron nitride nanosheets and development of a deep-UV photo-detector. Nanoscale. 2014;6(9):4577–82.
49. Meng JH, Zhang XW, Wang HL, Ren XB, Jin CH, Yin ZG, et al. Synthesis of in-plane and stacked graphene/hexagonal boron nitride heterostructures by combining with ion beam sputtering deposition and chemical vapor deposition. Nanoscale. 2015;7(38):16046–53.
50. Wang H, Zhang X, Liu H, Yin Z, Meng J, Xia J, et al. Synthesis of large-sized single-crystal hexagonal boron nitride domains on nickel foils by ion beam sputtering deposition. Adv Mater. 2015;27(48):8109–15.
51. Aldalbahi A, Feng P. Development of 2-D boron nitride Nanosheets UV photoconductive detectors. IEEE Trans Electron Devices. 2015;62(6):1885–90.
52. Zhou AF, Aldalbahi A, Feng P. Vertical metal-semiconductor-metal deep UV photodetectors based on hexagonal boron nitride nanosheets prepared by laser plasma deposition. Optical Mater Express. 2016;6(10):3286–92.
53. Rivera M, Velázquez R, Aldalbahi A, Zhou AF, Feng P. High Operating Temperature and Low Power Consumption Boron Nitride Nanosheets Based Broadband UV Photodetector. Sci Rep. 2017;7:42973.
54. Onuma T, Hazu K, Uedono A, Sota T, Chichibu SF. Identification of extremely radiative nature of AlN by time-resolved photoluminescence. Appl Phys Lett. 2010;96(6):061906.
55. Lin R, Zheng W, Chen L, Zhu Y, Xu M, Ouyang X, et al. X-ray radiation excited ultralong (> 20,000 seconds) intrinsic phosphorescence in aluminum nitride single-crystal scintillators. Nat Commun. 2020;11(1):1–8.
56. Zhu Y, Lin R, Zheng W, Ran J, Huang FJSB. Near vacuum-ultraviolet aperiodic oscillation emission of AlN films; 2020.
57. Li J, Oder TN, Nakarmi ML, Lin JY, Jiang HX. Optical and electrical properties of mg-doped p-type AlxGa1−xN. Appl Phys Lett. 2002;80(7):1210–2.
58. Li J, Nam KB, Nakarmi ML, Lin JY, Jiang HX. Band-edge photoluminescence of AlN epilayers. Appl Phys Lett. 2002;81(18): 3365–7.
59. Li J, Nam KB, Nakarmi ML, Lin JY, Jiang HX, Carrier P, et al. Band structure and fundamental optical transitions in wurtzite AlN. Appl Phys Lett. 2003;83(25):5163–5.
60. Nam KB, Li J, Nakarmi ML, Lin JY, Jiang HX. Deep ultraviolet picosecond time-resolved photoluminescence studies of AlN epilayers. Appl Phys Lett. 2003;82(11):1694–6.
61. Zhang JP, Chitnis A, Adivarahan V, Wu S, Mandavilli V, Pachipulusu R, et al. Milliwatt power deep ultraviolet light-emitting diodes over sapphire with emission at 278 nm. Appl Phys Lett. 2002;81(26):4910–2.
62. Li Y, Zheng W, Huang FJP. All-silicon photovoltaic detectors with deep ultraviolet selectivity. PhotoniX. 2020;1:1–11.
63. Li Y, Guo J, Zheng W, Huang F. Amorphous boron nitride for vacuum-ultraviolet photodetection. Appl Physics Lett. 2020;117(2):023504.
64. Rachko ZA, Valbis JA. Luminescence of Free and Relaxed Excitons in MgO. Physica Status Solidi (b). 1979;93(1): 161–6.
65. Remes Z, Petersen R, Haenen K, Nesladek M, D'Olieslaeger M. Mechanism of photoconductivity in intrinsic epitaxial CVD diamond studied by photocurrent spectroscopy and photocurrent decay measurements. Diam Relat Mater. 2005;14(3): 556–60.
66. Balducci A, Marinelli M, Milani E, Morgada ME, Tucciarone A, Verona-Rinati G, et al. Extreme ultraviolet single-crystal diamond detectors by chemical vapor deposition. Appl Phys Lett. 2005;86(19):193509.
67. Uchida K, Ishihara H, Nippashi K, Matsuoka M, Hayashi K. Measurement of vacuum ultraviolet radiation with diamond photo detectors. J Light Vis Eng. 2004;28(2):97.
68. Saito T, Hayashi K, Ishihara H, Saito I. Characterization of photoconductive diamond detectors as a candidate of FUV/ VUV transfer standard detectors. Metrologia. 2006;43(2):S51.
69. Richter M, Kroth U, Gottwald A, Gerth C, Tiedtke K, Saito T, et al. Metrology of pulsed radiation for 157-nm lithography. Appl Opt. 2002;41(34):7167–72.
70. Saito T, Hayashi K. Spectral responsivity measurements of photoconductive diamond detectors in the vacuum ultraviolet region distinguishing between internal photocurrent and photoemission current. Appl Phys Lett. 2005;86(12): 122113.
71. Liu Z, Ao J-P, Li F, Wang W, Wang J, Zhang J, et al. Fabrication of three dimensional diamond ultraviolet photodetector through down-top method. Appl Phys Lett. 2016;109(15):153507.
72. Shi X, Yang Z, Yin S, Zeng H. Al plasmon-enhanced diamond solar-blind UV photodetector by coupling of plasmon and excitons. Mater Technol. 2016;31(9):544–7.
73. Liu K, Dai B, Ralchenko V, Xia Y, Quan B, Zhao J, et al. Single crystal diamond UV detector with a groove-shaped electrode structure and enhanced sensitivity. Sens. Actuators, A. 2017;259:121–6.
74. Lin C-N, Lu Y-J, Yang X, Tian Y-Z, Gao C-J, Sun J-L, et al. Diamond-based all-carbon Photodetectors for solar-blind imaging. Adv Opt Mater. 2018;6(15):1800068.
75. Liu S, Ye J, Cao Y, Shen Q, Liu Z, Qi L, et al. Tunable hybrid Photodetectors with Superhigh Responsivity. Small. 2009; 5(21):2371–6.
76. Li L, Wu P, Fang X, Zhai T, Dai L, Liao M, et al. Single-crystalline CdS Nanobelts for excellent field-emitters and ultrahigh quantum-efficiency Photodetectors. Adv Mater. 2010;22(29):3161–5.
77. Fang X, Xiong S, Zhai T, Bando Y, Liao M, Gautam UK, et al. High-performance blue/ultraviolet-light-sensitive ZnSe-Nanobelt Photodetectors. Adv Mater. 2009;21(48):5016–21.

78. Alivisatos AP. Scaling law for structural metastability in semiconductor nanocrystals. Ber Bunsenges Phys Chem. 1997; 101(11):1573–7.
79. Huang F, Banfield JF. Size-dependent phase transformation kinetics in Nanocrystalline ZnS. J Am Chem Soc. 2005; 127(12):4523–9.
80. Zheng W, Lin R, Zhang Z, Huang F. Vacuum-ultraviolet Photodetection in few-layered h-BN. ACS Appl Mater Interfaces. 2018;10(32):27116–23.
81. Liao M, Koide Y, Alvarez J. Single Schottky-barrier photodiode with interdigitated-finger geometry: application to diamond. Appl Phys Lett. 2007;90(12):123507.
82. Almaviva S, Marinelli M, Milani E, Prestopino G, Tucciarone A, Verona C, et al. Extreme UV photodetectors based on CVD single crystal diamond in a p-type/intrinsic/metal configuration. Diam Relat Mater. 2009;18(1):101–5.
83. Almaviva S, Marinelli M, Milani E, Prestopino G, Tucciarone A, Verona C, et al. Extreme UV single crystal diamond Schottky photodiode in planar and transverse configuration. Diam Relat Mater. 2010;19(1):78–82.
84. Almaviva S, Marinelli M, Milani E, Prestopino G, Tucciarone A, Verona C, et al. Chemical vapor deposition diamond based multilayered radiation detector: Physical analysis of detection properties. J Appl Physics. 2010;107(1):014511.
85. Iwakaji Y, Kanasugi M, Maida O, Ito T. Characterization of diamond ultraviolet detectors fabricated with high-quality single-crystalline chemical vapor deposition films. Appl Phys Lett. 2009;94(22):223511.
86. Mirkarimi PB, McCarty KF, Medlin DL. Review of advances in cubic boron nitride film synthesis. Mater Sci Eng. 1997;21(2): 47–100.
87. Jiang X, Jia CL. Direct local Epitaxy of diamond on Si(100) and surface-roughening-induced crystal Misorientation. Phys Rev Lett. 2000;84(16):3658–61.
88. Feldermann H, Ronning C, Hofsäss H, Huang YL, Seibt M. Cubic boron nitride thin film heteroepitaxy. J Appl Phys. 2001; 90(7):3248–54.
89. Walker J. Optical absorption and luminescence in diamond. Rep Prog Phys. 1979;42(10):1605.
90. Pascallon J, Stambouli V, Ilias S, Bouchier D, Nouet G, Silva F, et al. Microstructure of c-BN thin films deposited on diamond films. Diam Relat Mater. 1999;8(2):325–30.
91. Kester DJ, Ailey KS, Lichtenwalner DJ, Davis RF. Growth and characterization of cubic boron nitride thin films. J Vac Sci Technol A. 1994;12(6):3074–81.
92. Zhang W, Bello I, Lifshitz Y, Chan KM, Meng X, Wu Y, et al. Epitaxy on diamond by chemical vapor deposition: a route to high-quality cubic boron nitride for electronic applications. Adv Mater. 2004;16(16):1405–8.
93. Zhang WJ, Meng XM, Chan CY, Chan KM, Wu Y, Bello I, et al. Interfacial study of cubic boron nitride films deposited on diamond. J Phys Chem B. 2005;109(33):16005–10.
94. Zhang WJ, Bello I, Lifshitz Y, Chan KM, Wu Y, Chan CY, et al. Thick and adherent cubic boron nitride films grown on diamond interlayers by fluorine-assisted chemical vapor deposition. Appl Phys Lett. 2004;85(8):1344–6.
95. Soltani A, Barkad HA, Mattalah M, Benbakhti B, Jaeger J-CD, Chong YM, et al. 193nm deep-ultraviolet solar-blind cubic boron nitride based photodetectors. Appl Phys Lett. 2008;92(5):053501.
96. Li J, Fan ZY, Dahal R, Nakarmi ML, Lin JY, Jiang HX. 200nm deep ultraviolet photodetectors based on AlN. Appl Phys Lett. 2006;89(21):213510.
97. BenMoussa A, Soltani A, Gerbedoen JC, Saito T, Averin S, Gissot S, et al. Developments, characterization and proton irradiation damage tests of AlN detectors for VUV solar observations. Nucl. Instrum. Methods Phys. Res., Sect. B. 2013; 312:48–53.
98. Tsai D-S, Lien W-C, Lien D-H, Chen K-M, Tsai M-L, Senesky DG, et al. Solar-blind Photodetectors for harsh electronics. Sci Rep. 2013;3:2628.
99. Pantha BN, Dahal R, Nakarmi ML, Nepal N, Li J, Lin JY, et al. Correlation between optoelectronic and structural properties and epilayer thickness of AlN. Appl Phys Lett. 2007;90(24):241101.
100. Nikishin S, Borisov B, Pandikunta M, Dahal R, Lin JY, Jiang HX, et al. High quality AlN for deep UV photodetectors. Appl Phys Lett. 2009;95(5):054101.
101. Tannous C, Leclerc G, Yelon A. Time-dependent photoconductivity in the presence of light-induced recombination: application to atactic polystyrene. J Phys Condens Matter. 1989;1(27):4367.
102. Shimakawa K, Inami S, Kato T, Elliott SR. Origin of photoinduced metastable defects in amorphous chalcogenides. Phys Rev B. 1992;46(16):10062–9.
103. Manikandan N, Asokan S. Signatures of an extended rigidity percolation in the photo-degradation behavior and the composition dependence of photo-response of Ge–Te–in glasses. J Non-Cryst Solids. 2008;354(31):3732–4.
104. BenMoussa A, Hochedez JF, Dahal R, Li J, Lin JY, Jiang HX, et al. Characterization of AlN metal-semiconductor-metal diodes in the spectral range of 44–360nm: photoemission assessments. Appl Phys Lett. 2008;92(2):022108.
105. BenMoussa A, Schühle U, Scholze F, Kroth U, Haenen K, Saito T, et al. Radiometric characteristics of new diamond PIN photodiodes. Meas Sci Technol. 2006;17(4):913–7.
106. BenMoussa A, Schühle U, Haenen K, Nesládek M, Koizumi S, Hochedez JF. PIN diamond detector development for LYRA, the solar VUV radiometer on board PROBA II. Physica Status Solidi (a). 2004;201(11):2536–41.
107. Zheng W, Lin R, Ran J, Zhang Z, Ji X, Huang F. Vacuum-Ultraviolet Photovoltaic Detector. ACS Nano. 2018;12(1):425–31.
108. Kim KS, Zhao Y, Jang H, Lee SY, Kim JM, Kim KS, et al. Large-scale pattern growth of graphene films for stretchable transparent electrodes. Nature. 2009;457:706.
109. Chi On C, Okyay AK, Saraswat KC. Effective dark current suppression with asymmetric MSM photodetectors in group IV semiconductors. IEEE Photon Technol Lett. 2003;15(11):1585–7.
110. Xu C, Du Z, Huang Y, Dong M, Lin R, Li Y, et al. Amorphous-MgGaO film combined with Graphene for vacuum-ultraviolet photovoltaic detector. ACS Appl Mater Interfaces. 2018;10(49):42681–7.
111. Dong M, Zheng W, Xu C, Lin R, Zhang D, Zhang Z, et al. Ultrawide-Bandgap amorphous MgGaO: nonequilibrium growth and vacuum ultraviolet application. Adv. Opt. Mater. 2019;7(3):1801272.
112. Wei M, Yao K, Liu Y, Yang C, Zang X, Lin L. A solar-blind UV detector based on Graphene-microcrystalline diamond Heterojunctions. Small. 2017;13(34):1701328.
113. Zheng W, Lin R, Zhang D, Jia L, Ji X, Huang F. Vacuum-ultraviolet photovoltaic detector with improved response speed and Responsivity via heating annihilation trap state mechanism. Adv. Opt. Mater. 2018;6(21):1800697.

114. Jia L, Zheng W, Lin R, Huang F. Ultra-high Photovoltage (2.45 V) Forming in Graphene Heterojunction via Quasi-Fermi Level Splitting Enhanced Effect. iScience. 2020;23(2):100818.
115. Zheng W, Lin R, Jia L, Huang F. Vacuum ultraviolet photovoltaic arrays. Photonics Res. 2019;7(1):98–102.
116. Xu X, Chen J, Cai S, Long Z, Zhang Y, Su L, et al. A real-time wearable UV-radiation monitor based on a high-performance p-CuZnS/n-TiO2 Photodetector. Adv Mater. 2018;30(43):1803165.
117. Michel J, Liu J, Kimerling LC. High-performance Ge-on-Si photodetectors. Nat Photonics. 2010;4(8):527–34.
118. Stolterfoht M, Wolff CM, Márquez JA, Zhang S, Hages CJ, Rothhardt D, et al. Visualization and suppression of interfacial recombination for high-efficiency large-area pin perovskite solar cells. Nat Energy. 2018;3(10):847–54.
119. Baker DN. How to cope with space weather. Science. 2002;297(5586):1486.
120. Mortet V, Soltani A. Impurity impact ionization avalanche in p-type diamond. Appl Phys Lett. 2011;99(20):202105.
121. Mortet V, Trémouilles D, Bulíř J, Hubík P, Heller L, Bedel-Pereira E, et al. Peculiarities of high electric field conduction in p-type diamond. Appl Phys Lett. 2016;108(15):152106.
122. Skukan N, Grilj V, Sudić I, Pomorski M, Kada W, Makino T, et al. Charge multiplication effect in thin diamond films. Appl Phys Lett. 2016;109(4):043502.
123. Hiraiwa A, Kawarada H. Figure of merit of diamond power devices based on accurately estimated impact ionization processes. J Appl Phys. 2013;114(3):034506.
124. Zoroddu A, Bernardini F, Ruggerone P, Fiorentini V. First-principles prediction of structure, energetics, formation enthalpy, elastic constants, polarization, and piezoelectric constants of AlN, GaN, and InN: comparison of local and gradient-corrected density-functional theory. Phys Rev B. 2001;64(4):045208.
125. Park CH, Cheong B-H, Lee K-H, Chang KJ. Structural and electronic properties of cubic, 2H, 4H, and 6H SiC. Phys Rev B. 1994;49(7):4485–93.
126. Dahal R, Al Tahtamouni TM, Fan ZY, Lin JY, Jiang HX. Hybrid AlN–SiC deep ultraviolet Schottky barrier photodetectors. Appl Phys Lett. 2007;90(26):263505.
127. Dahal R, Al Tahtamouni TM, Lin JY, Jiang HX. AlN avalanche photodetectors. Appl Phys Lett. 2007;91(24):243503.

Publisher's Note

Springer Nature remains neutral with regard to jurisdictional claims in published maps and institutional affiliations.

Submit your manuscript to a SpringerOpen journal and benefit from:

- ► Convenient online submission
- ► Rigorous peer review
- ► Open access: articles freely available online
- ► High visibility within the field
- ► Retaining the copyright to your article

Submit your next manuscript at ► springeropen.com